A&A 460, 29–36 (2006)
DOI: 10.1051/0004-6361:20065229

Astronomy & Astrophysics

Structure formation and CMBR anisotropy spectrum in the inflessence model

A. A. Sen[1], V. F. Cardone[2], S. Capozziello[3], and A. Troisi[3]

[1] Department of Physics and Astronomy, Vanderbilt University, Nashville, TN 37235, USA
[2] Dipartimento di Fisica "E.R. Caianiello", Università di Salerno and INFN, Sezione di Napoli, Gruppo Collegato di Salerno, via S. Allende, 84081 Baronissi (Salerno), Italy
e-mail: winny@na.infn.it
[3] Dipartimento di Scienze Fisiche, Università di Napoli and INFN, Sezione di Napoli, Compl. Univ. di Monte S. Angelo, Edificio G, via Cinthia, 80121 Napoli, Italy

Received 17 March 2006 / Accepted 23 June 2006

ABSTRACT

The inflessence model has recently been proposed in an attempt to explain both early inflation and present day accelerated expansion within a single mechanism. The model has been successfully tested against the Hubble diagram of Type Ia Supernovae, the shift parameter, and the acoustic peak parameter. As a further mandatory test, we investigate here structure formation in the inflessence model determining the evolution of matter density contrast $\delta \equiv \delta\rho_{\rm M}/\rho_{\rm M}$ in the linear regime. We compare the growth factor $D(a) \equiv \delta/a$ and the growth index $f(z) \equiv {\rm dln}\delta/{\rm dln}a$ to these same quantities for the successful concordance ΛCDM model with a particular emphasis on the role of the inflessence parameters (γ, z_Q). We also evaluate the anisotropy spectrum of the cosmic microwave background radiation (CMBR) to check whether the inflessence model may be in agreement with the observations. We find that, for large values of (γ, z_Q), structure formation proceeds in a similar way to that in the ΛCDM scenario, and it is also possible to nicely fit the CMBR spectrum.

Key words. cosmology: theory – large scale structure of Universe – cosmology: observations

1. Introduction

It is now widely accepted that we live in a spatially flat universe undergoing an accelerated expansion and made of ∼95% dark ingredients about which we know little. On the one hand, observations of the CMBR anisotropy spectrum (see, e.g., de Bernardis et al. 2000; Hanany et al. 2000; Spergel et al. 2003; and Page 2004 for a review) indicates that the total energy density attains the critical one so that the universe is spatially flat. On the other hand, the SNeIa Hubble diagram (Riess et al. 2004; Astier et al. 2006) is a clear signature of the cosmic speed-up of the universe expansion, hence discarding with a great degree of confidence the old standard picture of a matter-dominated universe. Finally, the matter power spectrum and the clustering properties of galaxies observed in large galaxy surveys (Pope et al. 2004; Cole et al. 2005) point towards the existence of dark matter suggesting that its density parameter $\Omega_{\rm M}$ is of the order of 0.3, far lower than the SCDM value $\Omega_{\rm M} = 1$, thus stressing the need of a further component to achieve the critical density. When combined together, this impressive set of observations motivates the entrance on the scene of a new player dominating the energy budget and driving the accelerated expansion. This elusive and mysterious component is referred to as dark energy.

Although the need for dark energy is clear, its nature and fundamental properties are completely unknown. The simplest candidate is the well-known cosmological constant Λ (Carroll et al. 1992; Sahni & Starobinski 2000), which perfectly matches a wide range of observations (Tegmark et al. 2003; Seljak et al. 2005), hence awarding the name of concordance model to the scenario based on Λ and cold dark matter (CDM). Despite this impressive success, the ΛCDM model is plagued by serious theoretical shortcomings, thus motivating the search for alternative schemes. This has opened the way to an overwhelming flood of papers proposing different models for explaining the cosmic speed-up and the CMBR anisotropy spectrum with proposals ranging from a dynamical Λ originating from a scalar field (dubbed quintessence) rolling down its self-interaction potential (see, e.g., Peebles & Rathra 2003 and Padmanabhan et al. 2003 for comprehensive reviews), to unified models of dark matter and dark energy such as the Chaplygin gas (Kamenshchik et al. 2001; Bilić et al. 2002; Bento et al. 2003) and the Hobbit models (Cardone et al. 2004), to braneworld inspired scenarios (Dvali et al. 2000; Lue et al. 2004) and higher order theories of gravity both in the metric (Capozziello 2002; Capozziello et al. 2003; Nojiri & Odintsov 2003; Carroll et al. 2004; Capozziello et al. 2005) and the Palatini (Vollick 2003; Meng & Wang 2003; Flanagan 2004; Allemandi et al. 2004; Capozziello et al. 2004; Amarzguioi et al. 2005) formulations. Although radically different in their theoretical aspects, all of these models are equally viable from the observational point of view, thus indicating that better quality data, higher redshift probes, or new tests are in order to break some of the degeneracies among different models.

It is worth noting that both current theoretical schemes and observational evidences predict that the evolutionary history of the universe comprises two periods of accelerated expansion, namely the inflationary epoch and the present day dark energy dominated phase. In both cases, the expansion is usually interpreted as the result of the presence of a negative pressure fluid dominating the energy budget. It is natural to wonder whether a single (effective) fluid may indeed be responsable for both periods of accelerated expansion. At the same time, this fluid

should be subdominant during the radiation and matter dominated epochs so as not to interfere with baryogenesis and structure formation. While it is quite difficult to theoretically formulate the properties of such a fluid, it is, on the contrary, clear what its phenomenological features are. Inspired by these considerations, some of us have recently proposed the *inflessence* model (Cardone et al. 2005). Based on a suitable Ansatz for the dependence of the energy density on the scale factor a, the inflessence scenario has been shown to be able to fit the SNeIa Hubble diagram, and also give correct values for the shift $\mathcal{R}$ (Bond et al. 1997; Wang & Mukherejie 2004) and acoustic peak $\mathcal{A}$ (Eisenstein et al. 2005) parameters. While this result gives an observational motivation for the model, inflessence is also well founded theoretically, since it can be interpreted both in terms of scalar field quintessence and as an effective model coming from fourth order theories of gravity.

Motivated by these observational and theoretical results, we extend the analysis of the inflessence model here by investigating structure formation in this scenario. Moreover, we also present a preliminary analysis of the CMBR anisotropy spectrum. Both these features are standard observables in cosmology nowadays, and it is therefore mandatory to check whether the inflessence model is able to survive these tests.

The structure of the paper is as follows. Section 2 briefly recalls the main features of the inflessence model and explains what the roles played by its characterizing parameters are. In Sect. 3, the evolution of matter density perturbations is studied in the linear regime, assuming that the inflessence fluid does not cluster on the subhorizon scale, which is indeed the case of most dark energy models. Section 4 is dedicated to a discussion of how the growth index depends on the inflessence parameters and the constraints that could possibly be extracted from a precise determination of this quantity. The CMBR anisotropy spectrum is evaluated in Sect. 5, while a summary of the results and the conclusions are presented in Sect. 6.

2. The inflessence model

The key ingredient is the following Ansatz for the inflessence energy density:

$$\rho(a) = \mathcal{N} a^{-3} \left(1 + \frac{a_I}{a}\right)^{\beta} \left(1 + \frac{a}{a_Q}\right)^{\gamma} \tag{1}$$

with a normalization constant $\mathcal{N}$, slope parameters (β, γ), and two scaling values of the scale factor $a_I \ll a_Q$. For later applications, it is convenient to rewrite Eq. (1) in terms of the redshift $z = 1/a - 1$ (having set $a_0 = 1$ with the subscript 0 denoting henceforth quantities evaluated at the present day, i.e. $z = 0$):

$$\rho(z) = \mathcal{N}(1+z)^3 \left(1 + \frac{1+z}{1+z_I}\right)^{\beta} \left(1 + \frac{1+z_Q}{1+z}\right)^{\gamma}, \tag{2}$$

having defined:

$$z_I = 1/a_I - 1, \tag{3}$$

$$z_Q = 1/a_Q - 1. \tag{4}$$

From Eq. (1), it is quite easy to see that the energy density of the inflessence fluid scales like that of dust matter ($\rho \sim a^{-3}$) in the range $a_I \ll a \ll a_Q$, so that, given typical values for (a_I, a_Q), the fluid follows matter for a large part of the universe history, while it scales differently only during the very beginning ($a \ll a_I$) and the present ($a \gg a_Q$) periods. Moreover, choosing $\beta = -3$, the fluid energy density remains constant for $a \ll a_I$, thus behaving like the usual cosmological constant Λ during the early epoch of the universe evolution. Finally, the slope parameter γ determines how the fluid energy density scales with a in the present epoch.

It is still more instructive to look at the equation of state (EoS) $w \equiv p/\rho$, where p is the fluid pressure. Using the continuity equation:

$$\dot{\rho} + 3H(\rho + p) = 0, \tag{5}$$

with the Hubble parameter $H = \dot{a}/a$ and inserting Eq. (1) into Eq. (5), after some algebra we get:

$$w = \frac{\beta}{3}\left(\frac{1+z}{2+z+z_I}\right) - \frac{\gamma}{3}\left(\frac{1+z_Q}{2+z+z_Q}\right). \tag{6}$$

It is worth noting that w does not depend either on γ or on z_Q for high values of z, which is to be expected looking at Eq. (6). On the contrary, these two parameters play a key role in determining the behavior of the EoS over the redshift range $(0, 100)$, which represents most of the history of the universe (in terms of time).

The role of the different quantities $(\beta, \gamma, z_I, z_Q)$ is better understood considering the asymptotic limits of the EOS. We easily get:

$$\lim_{z\to\infty} w(z) = \frac{\beta}{3}, \tag{7}$$

which shows that setting $\beta = -3$, the fluid EoS approaches that of the cosmological constant, i.e., $w_\Lambda = -1$, in the very early universe. In general, if we impose the constraint $\beta < -1$, we get a fluid having a negative pressure in the far past so that it is able to drive the accelerated expansion occurring during the inflationary epoch. It is therefore clear that z_I controls the transition towards the past asymptotic value, in the sense that the larger is z with respect to z_I, the smaller is the difference between $w(z)$ and its asymptotic limit $\beta/3$. This consideration suggests that z_I has to take quite high values (indeed, far greater than 10^3) since, for $z \gg z_I$, the universe is in its inflationary phase.

In the asymptotic future (i.e., $z \to -1$), we get:

$$\lim_{z\to -1} w(z) = -\frac{\gamma}{3} \tag{8}$$

so that the slope parameter γ determines the future evolution of the universe. For instance, for $\gamma = 3$, the universe finally ends in a de Sitter state (as for the concordance ΛCDM model), while a Big Rip occurs for $\gamma > 3$, as in phantom models (Caldwell 2002; Caldwell et al. 2003).

Let us now consider the present day value of w that turns out to be:

$$w_0 = \frac{\beta}{3(2+z_I)} - \frac{\gamma}{3}\left(\frac{1+z_Q}{2+z_Q}\right) \simeq -\frac{\gamma}{3}\left(\frac{1+z_Q}{2+z_Q}\right) \tag{9}$$

where, in the second line, we used the fact that z_I is very large. Given that $z_Q > 0$, to have a present day accelerated expansion, w_0 should be lower than $-1/3$ so that we get the constraint $\gamma > (2+z_Q)/(1+z_Q)$. Moreover, depending on the values of γ and z_Q, w_0 could also be smaller than w_Λ so that we may recover phantom-like models. The parameter z_Q then regulates the transition to the dark energy-like dominated period.

In summary, the inflessence fluid with energy density and EOS given by Eqs. (2) and (6) is able to drive the accelerated expansion of the universe during both the inflationary epoch and

the present day period. Therefore, such a fluid plays the role of both the *inflaton* and the *quintessence* scalar field, hence the motivation for the name *inflessence* (contracting the words *inflationary quintessence*).

A general comment is in order here. Although originally proposed as a phenomenological Ansatz for the energy density, the inflessence model could also be seen as an effective parametrization of the scale factor during the universe's expansion, which translates into the above scaling of $\rho(z)$ given the known behavior of the matter and radiation components. This equivalent representation is particularly interesting during the inflationary epoch. Indeed, if the inflessence fluid plays the role of the inflaton field, one should wonder whether its self-interaction potential is able to give rise to reheating. Discussing this issue is outside our aims, but we stress that considering the model as a parametrization of the scale factor rather than the energy density makes it possible to escape problems with reheating.

It is worth noting that, since ρ scales with a as the dust matter energy density for a long period of the universe history, the coincidence problem is partially alleviated. Indeed, the dark energy and the matter components track each other for a long period so that their near equality today turns out to be a consequence of the relatively recent change of the scaling of the inflessence energy density with a. However, there is still a certain degree of fine tuning since the model parameters have to be set in a suitable way so that the transition from decelerated to accelerated expansion takes place only recently. Moreover, although $w_0 < -1$ is possible depending on the values of (γ, z_Q), the possibility to avoid the Big Rip still remains if $\gamma \leq 3$, although such low values seem to be disfavored by the fitting to the dimensionless coordinate distance of SNeIa and radiogalaxies.

As a final important remark, let us stress that, although phenomenologically inspired, the inflessence model may also be theoretically well-founded. Indeed, as shown in Cardone et al. (2005), one could obtain Eq. (2) as a result of scalar field quintessence with a self-interacting potential, which can be well approximated as a simple power law with negative slope. As an alternative explanation, the inflessence model may also be recovered as the effective fluid like description of a fourth order $f(R)$ theory in which the Einsteinian gravity Lagrangian $f(R) \propto R$ is replaced by a suitably reconstructed $f(R)$. From a different point of view, this also offers the possibility of considering the inflessence scenario as an analytical parametrization for studying a wide class of diverse models. As such, investigating the growth of structures for the inflessence fluid gives indirect constraints on these models too. To this end, it is worth stressing that we are assuming that the inflessence model may be recovered as a particular case of scalar field quintessence so that the gravity Lagrangian is the standard one, and we can therefore resort to the usual perturbation theory for our analysis of the growth of structures. Should we choose the interpretation of the inflessence model in the framework of $f(R)$ theories, we should adopt a different formalism.

3. Linear growth of fluctuations

The inflessence model has been successfully tested against the SNeIa Hubble diagram, also taking into account the shift parameter (which essentially gives the distance to the last scattering surface) and the baryonic acoustic peak parameter. Although successfully fitting this dataset is mandatory for any realistic dark energy model, such a test only probes the dynamics of the background cosmology. Indeed, dark energy also has impacts on the evolution of density perturbations.

As is well known, the universe is homogenous and isotropic only on the largest scales. As a consequence, while one can still use the standard FRW description when considering the dynamics of the universe on the scales of interest, smaller scale evolution must take into account the inhomogeneities of the spacetime. Using the equations of motion for this perturbed metric, one can derive the growth of density perturbations. Moreover, it is possible to demonstrate that, because of its high sound speed, dark energy only clusters on scales that are far larger than those of galaxies and galaxy clusters. As a consequence, dark energy affects the structure formation process only because of its background energy density, which concurs to determine the expansion rate. This is indeed also the case for the inflessence model we are considering here, so that we may resort to the standard theory to investigate the growth rate of matter perturbations in the linear regime.

Denoting the matter density contrast with $\delta \equiv \delta\rho_{\rm M}/\rho_{\rm M}$, the perturbation equation reads:

$$\ddot{\delta} + 2H\dot{\delta} - 4\pi G\rho_{\rm M}\delta = 0. \tag{10}$$

It is convenient to change the variable from t to the scale factor a so that Eq. (10) may finally be rewritten as:

$$\delta'' + \left[\frac{3}{a} + \frac{(\ln E^2)'}{2}\right]\delta' - \frac{3\Omega_{\rm M}}{2E^2a^5}\delta = 0, \tag{11}$$

where the prime denotes the derivation with respect to the scale factor a and we have used $4\pi G\rho_{\rm M} = (3/2)\Omega_{\rm M}H_0^2a^{-3}$ and defined $E^2 = H^2/H_0^2$. To study the evolution of perturbations in the inflessence scenario, we have only to insert into Eq. (11) the corresponding expression for E^2, which reads:

$$E^2(a) = H^2(a)/H_0^2 = \Omega_{\rm r}a^{-4} + \Omega_{\rm M}a^{-3} + \Omega_{\rm X}g(a), \tag{12}$$

where $\Omega_{\rm r}$, $\Omega_{\rm M}$, and $\Omega_{\rm X}$ are the present day values of the density parameters for radiation, dust matter, and inflessence, respectively, and:

$$g(a) = a^{-3}\left(\frac{1 + a_I/a}{1 + a_I}\right)^{\beta}\left(\frac{1 + a/a_Q}{1 + 1/a_Q}\right)^{\gamma}. \tag{13}$$

Note that, consistent with the position of the first peak in the CMBR anisotropy spectrum, we have assumed a spatially flat universe so that $\Omega_{\rm r} + \Omega_{\rm M} + \Omega_{\rm X} = 1$, although some slight deviations from spatial flatness are still allowed by the data when a time-varying dark energy equation of state is used.

Since for a matter-only universe $\delta \propto a$, it is useful for studying the effect of dark energy to divide this behavior out and switch to the growth variable $D \equiv \delta/a$. Starting from Eq. (11), it is quite easy to determine the equation governing the evolution of this latter quantity[1]:

$$D'' + \left[\frac{5}{a} + \frac{(\ln E^2)'}{2}\right]D' + \left[\frac{3}{a}\left(1 - \frac{\Omega_{\rm M}}{2E^2a^3}\right) + \frac{(\ln E^2)'}{2}\right]\frac{D}{a} = 0. \tag{14}$$

Equation (14) may be solved analytically only in very special cases (see, e.g., Percival 2005 and references therein), while, for our model (and indeed for most of dark energy models), we have to resort to numerical integration using the boundary conditions $\dot{D} = 0$ and $D = 1$ as $a \to 0$. Actually, it

[1] Actually, one may also use $\ln a$ instead of a as expansion variable. See Linder (2005) for different equivalent equations to determine $D(a)$.

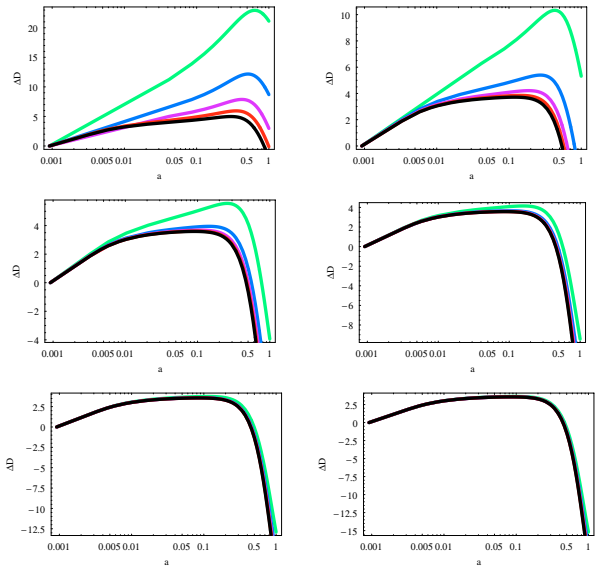

Fig. 1. ΔD vs. a for models with γ from 3.5 to 8.5 (in steps of 1) *from the top left to the bottom right panel*, and z_Q from 1.0 to 5.0 (in steps of 1) from the uppermost to the lowermost curve. The other parameters are set as explained in the text.

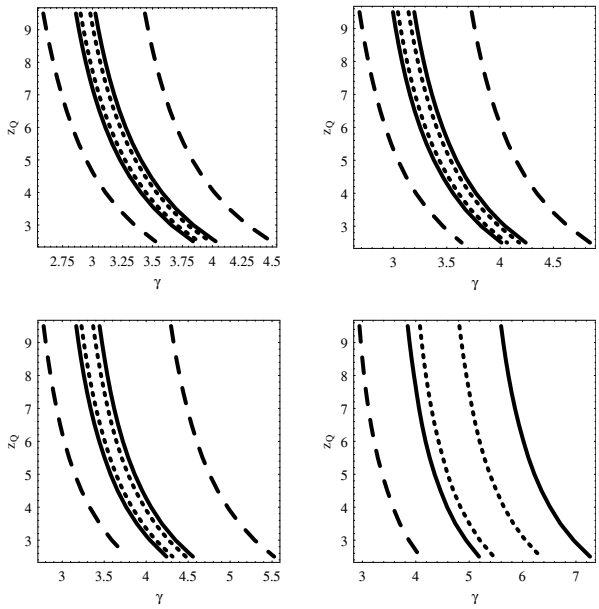

Fig. 2. Level contours for ΔD in the plane (γ, z_Q) at $z = 0$ (*top left*), 0.15 (*top right*), 0.35 (*bottom left*), and 1.0 (*bottom right*). Contours are plotted for $\Delta D = (\pm 0.5\%, \pm 1\%, \pm 5\%)$ with short-dashed, solid and long-dashed lines, respectively. Note that, for $z = 1.0$, the deviations are so small that the contour line at $\Delta D = 5\%$ lies outside the plot.

is not necessary to integrate from $a = 0$, but one may set $a = a_{\rm LS} = (1 + z_{\rm LS})^{-1}$ as the initial condition, $z_{\rm LS}$ being the redshift of the last scattering surface that we compute using the approximated relation in Hu & Sugyiama (1996). To this end, we set $\omega_{\rm b} = \Omega_b h^2 = 0.0214$ in accordance with the nucleosynthesis constraints (Kirkman et al. 2003) and $h = 0.664$ consistent with the Hubble diagram of low redshift SNeIa (Daly & Djorgovki 2004).

Rather than looking at $D(a)$ directly, it is more interesting to consider the quantity $\Delta D \equiv 1 - D/D_\Lambda$, which represents the percentage deviation of the growth factor for the inflessence model with respect to that for the concordance ΛCDM one. Figure 1 shows ΔD (multiplied by 100 for sake of clarity) as a function of the scale factor a for different combinations of the inflessence parameters (γ, z_Q), having set $(\Omega_{\rm M}, \Omega_{\rm r}) = (0.28, 9.89\times10^{-5})$ (for both the inflessence and the ΛCDM model) and fixed (β, z_I) to their fiducial values $(-3, 3454)$ (Cardone et al. 2005). Note that these latter parameters play a negligible role in our analysis since they mainly affect the evolution of the fluid in the very early inflationary epoch. It is worth stressing that setting $z_I = 3454$ does not at all mean that we are assuming that inflation took place for z near this value. On the contrary, as could be easily checked, the universe undergoes inflation only for $z \gg z_I$ so that the exact value of this latter parameter does not set the end of any inflationary period, which could lead to possible problems with nucleosynthesis.

Not surprisingly, the evolution of the growth factor highly depends on the values of the parameters (γ, z_Q), and both negative and positive deviations from the growth factor in the ΛCDM model may be obtained. Nevertheless, some general results may be inferred. First, we note that, although deviations as large as 20% may be obtained, for most of the parameter space (γ, z_Q) the growth factor of the inflessence model is comfortably similar to the ΛCDM one over the range $0.5 \le a \le 1$, i.e., $0 \le z \le 2$, where structure formation mainly occurs. Although detailed numerical simulations should be performed, this preliminary result makes us confident that the assembly of galaxies and clusters of galaxies should have taken place in a way that is quite similar to the one in the ΛCDM model.

Figure 1 also shows that, for a fixed a, the behavior of ΔD with z_Q depends on what the value of γ is. For instance, a better agreement with the ΛCDM model prediction is achieved for higher z_Q if $\gamma \le 4.5$, while the opposite is true for $\gamma \ge 7.5$. Actually, ΔD turns out to depend only weakly on z_Q for $\gamma > 4.5$ so that it is this latter parameter that mainly determines the behavior of the growth factor D with a in such a regime. To better investigate how ΔD depends on (γ, z_Q), it is therefore interesting to look at the contours of equal ΔD in the (γ, z_Q) plane, which are plotted in Fig. 2 for some representative values of the redshift z. Consider, for instance, the results for $z = 0.15$ (top right panel in Fig. 2). To have $|\Delta D| \le 5\%$, larger values of z_Q are markedly preferred only if coupled with low values of γ, while $z_Q \sim 3$ is allowed, provided that γ stays in the range $(3.7, 4.7)$. As a general rule, the lower the value of z_Q is, the γ higher must be to still have $|\Delta D| \le 5\%$. With this caveat in mind, we note, however, that, unless one chooses $z_Q > 5$ (which is rejected by the SNeIa fit), $\gamma \le 3$ is disfavored by the requirement that the evolution of density perturbations in the inflessence model mimicks that in the ΛCDM one within 5% over the range $0 \le z \le 1$. In particular, remembering Eq. (8), we argue that models in which the universe ends with a Big Rip are preferred.

It is interesting to note that fitting the SNeIa Hubble diagram with priors on the shift and acoustic peak parameters gives $3.17 \le \gamma \le 5.86$ and $z_Q \le 5.3$ at the 95% confidence level (Cardone et al. 2005). Although the best fit values $(\gamma, z_Q) = (3.73, 0.1)$ are likely to be excluded because of the large values of ΔD, it is nevertheless possible to find values of (γ, z_Q) that make it possible both to fit the kinematic data and give rise to an evolution of the structure as similar as possible to that in the concordance ΛCDM model.

It is worth noting that the above results could be qualitatively explained considering the properties of the inflessence fluid. As explained in the previous section, the energy density tracks that of matter (i.e., $\rho \propto a^{-3}$) for $z_Q \ll z \ll z_I$, while, for $z \ll z_Q$, $\rho \propto (1 + z)^{3-\gamma}$. A large value of z_Q means that the tracking of

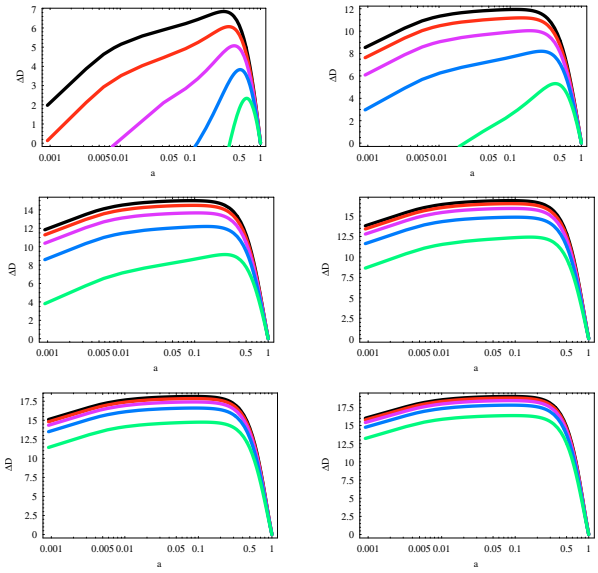

Fig. 3. Same as Fig. 1, but now D is normalized to D_Λ at the present day and the curves in each panel refer to z_Q from 1.0 to 5.0, from the lowermost to the uppermost.

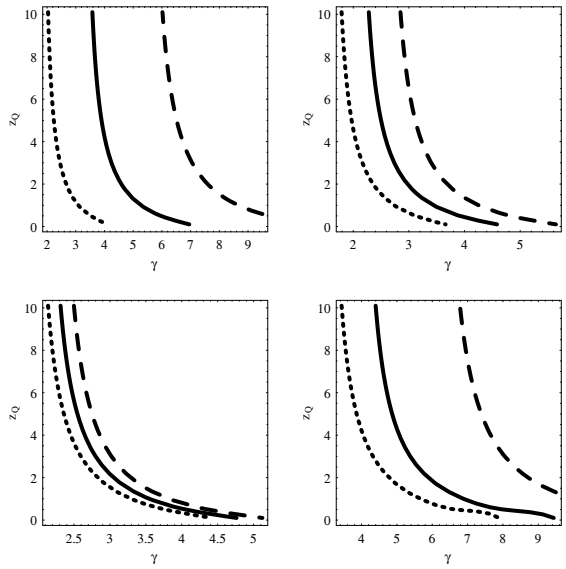

Fig. 4. Level contours for ΔD in the plane (γ, z_Q) at $z = 0.15$ (*top left*), 0.35 (*top right*), 1.0 (*bottom left*), and 1000 (*bottom right*). Contours are plotted for $\Delta D = (1\%, 2\%, 3\%)$ with short-dashed, solid, and long-dashed lines, respectively, in the first three panels, while $\Delta D = (5\%, 10\%, 15\%)$ are used for $z = 1000$.

matter is achieved only at high redshift when the dark energy density has become negligible with respect to that of matter. For this same reason, high values of γ are preferred since it allows ρ_X to increase with z at a slower rate with respect to ρ_M. As a general rule, the preferred values of (γ, z_Q) are those that render the inflessence energy density negligible with respect to the matter density during the structure formation epoch. This is the same mechanism achieved in the concordance ΛCDM model, thus explaining the shape of the contours of equal ΔD in the (γ, z_Q) plane.

The growth factor D could also be normalized to the present day value for the ΛCDM model, i.e., by setting $D(1) = D_\Lambda(1)$. Such an approach may be motivated considering that structure formation is in remarkably good agreement with the observations on the low redshift large-scale structure of the universe. By normalizing to this model at present, we may better investigate how the growth factor deviates from the ΛCDM one in the past. Figure 3 shows ΔD (as defined above) as a function of a for different values of the model parameters (γ, z_Q). Comparing Figs. 1 and 3, we immediately see that now ΔD is positive (i.e., $D(a) < D_\Lambda$) over the full range explored, whatever the values adopted for (γ, z_Q) are. Moreover, ΔD is an increasing function of both γ and z_Q for a given a, although the dependence on z_Q turns out to be quite weak for larger values of γ. To better investigate how ΔD depends on the model parameters, we plot the contours of equal ΔD in Fig. 4 for some representative values of the redshift z. As expected, at low redshift, the deviations are so small that a large part of the parameter space gives rise to a growth factor consistent (to well within ∼5%) with the one for the ΛCDM model, so that it is likely that structure formation takes place in the same way. Not surprisingly, such a region shrinks as the redshift increases as ΔD gets higher. Nevertheless, at $z = 1000$, $\Delta D < 15\%$ over almost the full parameter space considered.

Although an analytical solution of Eq. (14) is not available and numerical integration is straightforward, we believe it is useful to have an approximate expression for $D(a)$ to be used in data fitting. To this aim, we have integrated Eq. (14) for $a_{LS} \le a \le 1$, and found that a very good approximation is given by the fitting formula:

$$D(a) \simeq d_0 e^{\alpha\eta} \left(1 + d_1\eta + d_2\eta^2 + d_3\eta^3\right), \tag{15}$$

with $\eta = \ln a$, $d_0 = D(a = 1)$, and (α, d_1, d_2, d_3) constant parameters depending on (Ω_M, γ, z_Q). Equation (15) works very well with an rms error smaller than 2% up to $z \simeq 400$ and less than 8% at $z = 1100$. Unfortunately, we have not been able to find satisfactory approximated formulae for (α, d_1, d_2, d_3) in terms of (Ω_M, γ, z_Q), although we have generated tables (available on request to the authors) for $0.05 \le \Omega_M \le 0.55$, $2.5 \le \gamma \le 7.5$ and $0.1 \le z_Q \le 7.1$, which may be easily interpolated to get the corresponding fitting parameters. As an example, we report their values in Table 1 for some interesting cases.

Table 1. Values of the fitting parameters in Eq. (15) for some representative sets of (Ω_M, γ, z_Q). The first row refers to the best fit to SNeIa fit, while the remaining rows refer to models providing a good fit to the CMBR anisotropy spectrum.

Ω_M, γ, z_Q	α	d_1	d_2	d_3
0.28, 3.7, 0.1	0.1355	−0.5725	−0.0471	−0.0124
0.24, 5.0, 4.0	0.3371	−0.6510	−0.0878	−0.0367
0.24, 5.5, 5.0	0.3474	−0.6275	−0.0814	−0.0377
0.24, 6.0, 7.0	0.3513	−0.5983	−0.0731	−0.0372

4. Growth index

A quantity that can be measured by the galaxy correlation function or the peculiar velocities is the so-called *growth index* defined as:

$$f \equiv \frac{\mathrm{d}\ln\delta}{\mathrm{d}\ln a} = \frac{a}{\delta}\frac{\mathrm{d}\delta}{\mathrm{d}a}. \tag{16}$$

From a theoretical point of view, to estimate f for a given dark energy model, one may solve Eq. (11) to get $\delta = \delta(a)$ and then

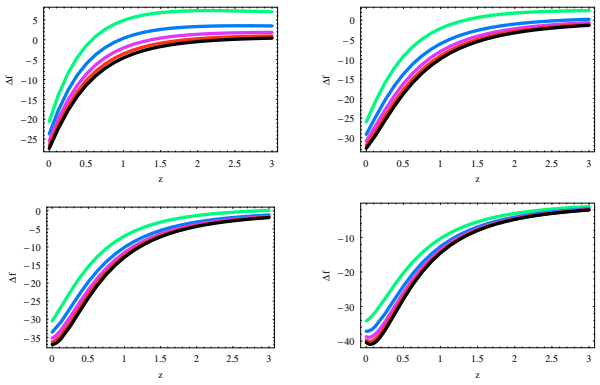

Fig. 5. Δf vs. z for models with $\gamma = 3.5$ (*top left*), 4.5 (*top right*), 5.5 (*bottom right*), and 6.5 (*bottom right*) and z_Q from 1.0 to 5.0 (in steps of 1) from the uppermost to the lowermost curves. The other parameters are set as explained in the text.

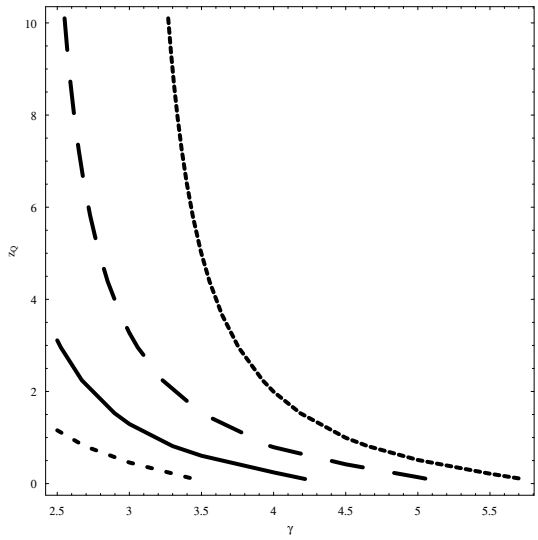

Fig. 6. Level contours for Δf at $z = 0.15$ in the plane (γ, z_Q). Contours are plotted for $\Delta f(z = 0.15) = -5\%$ (short-dashed), -10% (solid), and -15% (long-dashed). Models lying to the left of the dotted line have $w_0 \geq -1$, while the ones to the right behave today as phantoms, i.e., $w_0 < -1$.

straightforwardly compute f. However, since we often have to deal with numerical integration, it is better to directly solve an equation for f, to avoid propagating the numerical errors. To this end, one should simply use definition (16) of f and multiply Eq. (11) by a/δ to finally get the evolution equation for the growth index:

$$f' + \frac{f^2}{a} + \left[\frac{2}{a} + \frac{(\ln E^2)'}{2}\right] f - \frac{3\Omega_{\rm M}}{2E^2 a^4} = 0. \tag{17}$$

Not surprisingly, Eq. (17) must be integrated numerically, using $f(a_{\rm LS}) = 1$ as the initial condition, and Eqs. (12) and (13) for the particular case of the inflessence model.

The 2dFGRS collaboration measured the position and the redshift of over 220 000 galaxies and, from the analysis of the correlation function, determined the redshift distortion parameter f/b with the bias parameter b quantifying the difference between the galaxies and dark haloes distributions. Using the estimated f/b and the two different methods employed by Verde et al. (2001) and Lahav et al. (2002) to determine the bias b, one may estimate $f = 0.51 \pm 0.1$ or $f = 0.58 \pm 0.11$ at the survey effective depth $z = 0.15$.

Both of these estimates are in very good agreement with what is predicted by the ΛCDM model, so that it is interesting to compare the behaviour of f predicted by the inflessence model with that of the concordance scenario. To this end, we define $\Delta f = 1 - f/f_\Lambda$, which gives the percentage difference between the predictions of the two models. This is shown in Fig. 5, multiplied by 100 for the sake of clarity, considering different values of γ and z_Q and setting the other parameters as in Sect. 3. It is worth noting that Δf is always negative, i.e. the growth index f of the inflessence model is larger than the ΛCDM one over the whole parameter space (γ, z_Q). It is therefore mandatory to directly compare $f(z = 0.15)$ with the observed value (which is in good agreement with the concordance model predictions) to check whether the overestimate of f may be troublesome thus allowing us to put constraints on the parameter space.

As in the case of ΔD, the dependence of Δf on the model parameters (γ, z_Q) is particularly involved, so that it is better to look at the contours of equal Δf in the plane (γ, z_Q). These are shown in Fig. 6, where we have set $z = 0.15$ to compare with the observed value of f measured by the SDSS survey. It is worth noting that such a plot could be used to constrain (γ, z_Q) by requiring that $\Delta f(z = 0.15)$ be lower than a given threshold dictated by the estimated f. It is clear that such a method has the potential to severely narrow the region of the parameter space (γ, z_Q) in agreement with the observations. Moreover, a comparison of Fig. 6 with the projected likelihood contours from the SNeIa Hubble diagram fitting shows that they are orthogonal, so that a combined analysis may place strong constraints on the inflessence model parameters. Unfortunately, this method is still not applicable at the moment because the estimated f is still affected by a large percentage error (∼20%), which makes the test useless, since, as Fig. 6 shows, $\Delta f \leq 15\%$ over a wide region of the (γ, z_Q) plane. This is essentially due to the low redshift tested ($z = 0.15$), but extending the measurement to higher z (also with the same percentage error) could significantly improve the efficiency of such an analysis. Nevertheless, it is worth noting that the allowed region of the parameter space (γ, z_Q) lies to the left of the $w = -1$ line so that phantom like models are excluded. Such a result is nicely consistent with the constraints from the SNeIa fit that also point towards this conclusion.

Using the definitions of D and f, one easily gets:

$$f = D\left(1 + \frac{1}{D}\frac{{\rm d}\ln D}{{\rm d}\ln a}\right) \tag{18}$$

so that f not only depends on how density perturbations evolve, but also on their logarithmic rate of evolution. As such, f is a more subtle quantity depending on both the expansion history and the structure evolution. As a general remark, we note that Δf approaches null values more quickly than ΔD as a consequence of its logarithmic nature. It is nevertheless interesting to compare the contours of equal ΔD with those of equal Δf to see whether narrower constraints on the model parameters (γ, z_Q) may be obtained by imposing the same threshold on both quantities. Indeed, although the contours turn out to be parallel, they are also shifted towards each other so that the overlapping region is significantly narrower than those selected by the constraint on Δf alone. Should we have an observationally motivated constraint on ΔD (as that on Δf) to the 5% level of precision, we could thus efficiently constrain the inflessence parameters (γ, z_Q).

Indeed, it is likely that future measurements (using a larger redshift survey observing more galaxies) should lessen the error

on the observed $f(z = 0.15)$ to the 5% level. In such a case, it would be useful to have an approximated formula for $f(z = 0.15)$ as a function of the inflessence model parameters. This is given as:

$$f(z = 0.15) \simeq f_0 \Omega_{\rm M}^{f_1 + f_2 \ln\gamma + f_3 \ln z_Q} \qquad (19)$$

with:

$$(f_0, f_1, f_2, f_3) = (0.8778, 0.4614, -0.1839, -0.0323),$$

which works quite well (with an rms error less than 1.5%) for $0.2 \leq \Omega_{\rm M} \leq 0.4$, $3 \leq \gamma \leq 6$ and $1 \leq z_Q \leq 7$. It is worth noting that, for the ΛCDM model, one has the approximated formula $f_\Lambda(z) \simeq \left[\Omega_{\rm M}(1+z)^3\right]^{0.55}$ (Silveira & Waga 1994; Wang & Steinhardt 1998; Lokas et al. 2004). For the inflessence model, we find a similar formula, but the value of the exponent is determined by the model parameters (γ, z_Q). Note, however, that Eq. (19) only holds for $z = 0.15$. Although we have not explicitly checked it, it is likely that the same formal expression holds over a large range in z, provided that the parameters (f_0, f_1, f_2, f_3) are suitably changed.

5. CMBR anisotropy spectrum

Since its discovery by Penzias & Wilson (1965), the CMBR has played a fundamental role in cosmology. The recent precise measurement of its anisotropy spectrum by the WMAP collaboration (Spergel et al. 2003) has further increased the importance of such an observable in assessing the viability of any cosmological model. Unfortunately, the large number of parameters entering the determination of the anisotropy spectrum makes it quite difficult to extract constraints on a given model's parameters from a time-expensive likelihood analysis (typically based on a Monte Carlo Markov Chain exploration of the wide parameter space). This is also the case for the inflessence model, so that we will only investigate how the spectrum changes as a function of the main model parameters, i.e., (γ, z_Q). In the following analysis, we therefore set the following values for the other parameters involved in the computation:

$$\omega_{\rm b} = 0.04,\ \Omega_{\rm M} = 0.24,\ h = 0.70,\ \tau = 0.17,\ n = 1$$

with the optical depth τ and the spectral index (assuming no running) n. The remaining inflessence parameters (β, z_I) are set to their fiducial values $(-3, 3454)$. To compute the CMBR anisotropy spectrum, we use CMBFAST (Seljak & Zaldarriaga 1996), obtaining the results plotted in Figs. 7 and 8, where the inflessence parameters (γ, z_Q) has been chosen with the main aim of highlighting the dependence on these parameters rather than providing a good fit to the data.

As in the case of the growth factor D, large values of both γ and z_Q are needed to get satisfactory results. Indeed, while the position of the peaks is essentially independent on the parameters (γ, z_Q), their amplitude is an incresing function of these two quantities. Moreover, at the low multipoles ($l \leq 10$), the spectrum is significantly overestimated for small values of the inflessence parameters. It is worth stressing, however, that very good fits may be achieved by suitably tuning the parameters (γ, z_Q). Some nice examples are shown in Fig. 9.

It is worth noting that such large values of (γ, z_Q) stay at the upper end of the confidence ranges obtained from the likelihood analysis performed in Cardone et al. (2005). Nevertheless, they are not excluded, so that we are confident that a combined analysis of the whole parameter space (thus also changing the matter density parameter $\Omega_{\rm M}$ that we have held fixed up to now, the

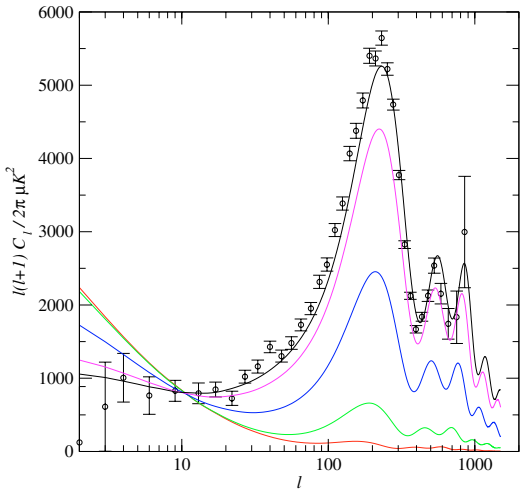

Fig. 7. The CMBR anisotropy spectrum for the inflessence model with $z_Q = 0.1$ and $\gamma = 3, 4, 5, 6, 7$ (from bottom to top). Other parameters are set as explained in the text. Data points are the WMAP measurements.

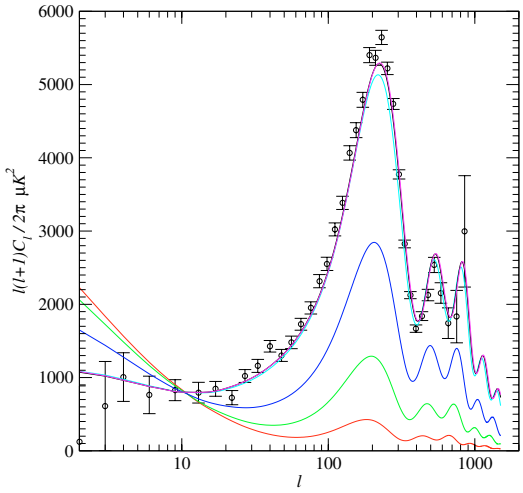

Fig. 8. The CMBR anisotropy spectrum for the inflessence model with $\gamma = 3.73$ and $z_Q = 0.1, 0.5, 1, 3, 5$ (from *bottom* to *top*). Other parameters are set as explained in the text. Data points are the WMAP measurements.

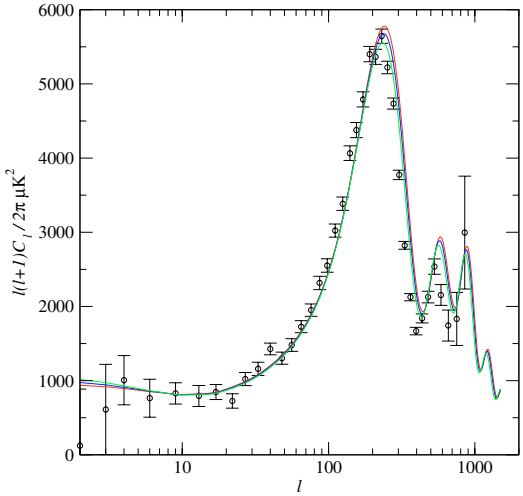

Fig. 9. The CMBR anisotropy spectrum for the inflessence model with $(\gamma, z_Q) = (6, 7)$, $(5.5, 5)$, and $(5, 4)$, from *top* to *bottom*. Other parameters are set as explained in the text. Data points are the WMAP measurements.

spectral index n, and the optical depth τ) could pinpoint a narrow region in the parameter space giving a satisfactory fit to SNeIa Hubble diagram, growth index, and CMBR anisotropy spectrum.

6. Conclusions

The inflessence model has been proposed as a possible mechanism to explain both the inflationary epoch in the early universe and the present day cosmic speed up. According to this scenario, a single fluid with the energy density given by Eq. (1) is added to radiation and dust matter, thus working as the inflaton field at very low a (i.e., for $z \gg z_I$) and as dark energy on the scale $a \sim 1$ (namely, for $z \leq z_Q$). Since this model has been shown to be able to nicely fit the SNeIa Hubble diagram, while also giving correct values for the shift and acoustic peak parameters, it is worth wondering how structure formation takes place.

To this end, we have investigated the evolution of density perturbations in the linear regime, comparing both the growth factor $D(a)$ and the growth index $f(z)$ to these same quantities in the ΛCDM model. In particular, we have concentrated our attention on the two inflessence parameters γ and z_Q, which determine, respectively, the asymptotic value of the eos (and hence the final fate of the universe) and the transition from the matter like to the quintessence like scaling of the energy density with a. Moreover, since γ and z_Q also set the present day value of the EoS, one can easily understand that they play a leading role in determining both $D(a)$ and $f(z)$. As a further test, we have also computed the CMBR anisotropy spectrum for fixed values of the other parameters (especially the optical depth τ and the spectral index n).

As a general result, we have found that, using large values of γ and z_Q, it is possible to work out scenarios in which structure formation takes place in quite similar ways in both the inflessence and the ΛCDM models. Moreover, for these same values, the predicted CMBR anisotropy spectrum also nicely agrees with the WMAP data. Such large values seem to be disfavored by the fitting to the SNeIa Hubble diagram, so that some tension between these two different probes is present. However, it is worth noting that the constraints coming from SNeIa are rather weak so that it is indeed possible that such a conflict is not particularly worrisome.

It is also worth noting that a precise determination of the growth index f (at the 5−10% level) at the low redshift typical of present day galaxy surveys or a measurement of f at a higher redshift have the potential to severely constrain the parameters (γ, z_Q). Moreover, such constraints are orthogonal to those coming from SNeIa, so that a joint analysis could definitively assess the viability of the inflessence model and pinpoint a narrow range in the parameter space $(\Omega_{\rm M}, \gamma, z_Q)$. One could also include the CMBR anisotropy spectrum in a fully comprehensive likelihood test. However, such an approach is likely to be affected by strong degeneracies among the five inflessence parameters $(\Omega_{\rm M}, \beta, \gamma, z_I, z_Q)$ and the other CMBR parameters such as the optical depth τ, the baryon content $\omega_{\rm b}$, and the spectral index n (and its eventual running $\mathrm{d}n/\mathrm{d}\ln k$). To probe such a large parameter space, a Monte Carlo Markov Chain approach is mandatory and is left for future works.

Actually, having determined the growth factor $D(a)$, for which we have also found an analytical approximation, we may further explore the issue of structure formation in the inflessence model. To this aim, one could use the estimated $D(a)$ to estimate the critical overdensity for collapse at the present day, and as a function of time, hence determining the mass function through the Press & Schechter formalism (Press & Schechter 1974) for the spherical collapse of perturbations, or its generalization to elliptical collapse worked out by Sheth and Tormen (1999). The mass function is the key ingredient to predicting cluster number counts, which are known to be a powerful test of dark energy models (see, e.g., Haiman et al. 2001). In many observational applications, it is also interesting to check whether the collapsed perturbation is virialized or not. As has been pointed out in Percival (2005), dark energy also plays a role in this process, and hence it is interesting to investigate how the inflessence model affects this important process. Most of these problems will be addressed in a forthcoming paper.

References

Allemandi, G., Borowiec, A., & Francaviglia, M. 2004, Phys. Rev. D, 70, 043524
Amarzguioi, M., Elgaroy, O., & Mota, D. F., Multamaki, T. 2005, [arXiv:astro-ph/0510519]
Astier, P., Guy, J., Regnault, N., et al. 2006, A&A, 447, 31
Bento, M. C., Bertolami, O., & Sen, A. A. 2003, Phys. Rev. D, 67, 063003
Bilić, N., Tupper, G. B., & Viollier, R. D. 2002, Phys. Lett. B, 535, 17
Bond, J. R., Efstathiou, G., & Tegmark, M. 1997, MNRAS, 291, L33
Caldwell, R. R. 2002, Phys. Lett. B, 545, 23
Caldwell, R. R., Kamionkowski, M., & Weinberg, N. N. 2003, Phys. Rev. Lett., 91, 071301
Capozziello, S. 2002, Int. J. Mod. Phys. D, 11, 483
Capozziello, S., Cardone, V. F., Carloni, S., & Troisi, A. 2003, Int. J. Mod. Phys. D, 12, 1969
Capozziello, S., Cardone, V. F., & Francaviglia, M. 2004, Gen. Rel. Grav., in press [arXiv:astro-ph/0410135]
Capozziello, S., Cardone, V. F., & Troisi A. 2005, Phys. Rev. D, 71, 043503
Cardone, V. F., Troisi, A., & Capozziello, S. 2004, Phys. Rev. D, 69, 083517
Cardone, V. F., Troisi, A., & Capozziello, S. 2005, Phys. Rev. D, 72, 043501
Carroll, S. M., Press, W. H., & Turner, E. L. 1992, ARA&A, 30, 499, 1992
Carroll, S. M., Duvvuri, V., Trodden, M., & Turner, M. 2004, Phys. Rev. D, 70, 043528
Cole, S., Percival, W. J., Peacock, J. A., et al. 2005, MNRAS, 362, 505
Daly, R. A., & Djorgovski, S. G. 2004, ApJ, 612, 652
de Bernardis, P., Ade, P. A. R., Bock, J. J., et al. 2000, Nature, 404, 955
Dvali, G. R., Gabadadze, G., & Porrati, M. 2000, Phys. Lett. B, 485, 208, 2000
Eisenstein, D., Zehavi, I., Hogg, D. W., et al. 2005, ApJ, 633, 560
Flanagan, E. E. 2004, Class. Quant. Grav., 21, 417
Haiman, Z., Mohr, J. J., & Holder, G. P. 2001, ApJ, 553, 545
Hanany, S., Ade, P., Balbi, A., et al. 2000, ApJ, 545, L5
Hu, W., & Sugyiama, N. 1996, ApJ, 471, 542
Kamenshchik, A., Moschella, U., & Pasquier, V. 2001, Phys. Lett. B, 511, 265
Kirkman, D., Tyler, D., Suzuki, N., O'Meara, J. M., & Lubin, D. 2003, ApJS, 149, 1
Lahav, O., Bridle, S. L., Percival, W. J., et al. 2002, MNRAS, 333, 961
Linder, E. V. 2005, Phys. Rev. D, 72, 043529
Lokas, E. L., Bode, P., & Hoffman, Y. 2004, MNRAS, 349, 595
Lue, A., Scoccimarro, R., & Starkman, G. 2004, Phys. Rev. D, 69, 124015
Meng, X. H., & Wang, P. 2003, Class. Quant. Grav., 20, 4949
Nojiri, S., & Odintsov, S. D. 2003, Phys. Lett. B, 576, 5
Padmanabhan, T. 2003, Phys. Rep., 380, 235
Page, L. A. 2004, [arXiv:astro-ph/0402547]
Peebles, P. J. E., & Rathra, B. 2003, Rev. Mod. Phys., 75, 559
Penzias, A. A., & Wilson, R. W. 1965, ApJ, 142, 419
Percival, W. 2005, A&A, 443, 819
Pope, A. G., Matsubara, T., Szalay, A. S., et al. 2004, ApJ, 607, 655
Press, W., & Schechter, P. L. 1974, ApJ, 187, 425
Riess, A. G., Strolger, L.-G., Tonry, J., et al. 2004, ApJ, 607, 665
Sahni, V., & Starobinski, A. 2000, Int. J. Mod. Phys. D, 9, 373
Seljak, U., & Zaldarriaga, M. 1996, ApJ, 469, 437
Seljak, U., Makarov, A., McDonald, P., et al. 2005, Phys. Rev. D, 71, 103515
Sheth, R. K., & Tormen, G. 1999, MNRAS, 108, 119
Silveira, V., & Waga, I. 1994, Phys. Rev. D, 50, 4890
Spergel, D. N., Verde, L., Peiris, H. V., et al. 2003, ApJS, 148, 175
Tegmark, M., Strauss, M. A., Blanton, M. R., et al. 2004, Phys. Rev. D, 69, 103501
Verde, L., Kamionkowski, M., Mohr, J. J., & Benson, A. J. 2001, MNRAS, 321, L7
Vollick, D. N. 2003, Phys. Rev., 68, 063510
Wang, L., & Steinhardt, P. J. 1998, ApJ, 508, 483
Wang, Y., & Mukherjee, P. 2004, ApJ, 606, 654